crystals

MDPI

Article

The Application of Organic Phosphate Nucleating Agents in Polypropylene with Different Molecular Weights

Juan Li [1], Zhaohua Liang [2], Chengtao Gao [1], Shanshan Luo [1], Shaowen Huang [1], Daohai Zhang [1,3,*] and Shuhao Qin [1,*]

[1] National Engineering Research Center for Compounding and Modification of Polymer Materials, Guiyang 550014, China; shadowlijuan@163.com (J.L.); chengtaogao@163.com (C.G.); luoshanshanpoly@163.com (S.L.); 13824478040@163.com (S.H.)
[2] Guizhou Tire Co., Ltd., Guiyang 550003, China; liangzhaohua2019@163.com
[3] School of Chemical Engineering, Guizhou Minzu University, Guiyang 550000, China
* Correspondence: zhangdaohai6235@163.com (D.Z.); pec.shqin@gzu.edu.cn (S.Q.)

Abstract: Two kinds of organic phosphate nucleating agent (NA-11 and NA-21) were used in PP with different molecular weights through the melt extrusion method. The dispersibility of the nucleating agents in PP, and the effect of the nucleating agents on the molecular weight, rheological behavior and crystallization behavior of PP were investigated. SEM and TEM analysis showed that the average radius of the dispersed particles (nucleating agents) was larger in LPP than that in HPP. The good dispersion of NA-21 also created more nucleation embryos for the adsorption of polypropylene molecules than the agglomerated NA-11. The gel permeation chromatography (GPC) analysis showed that the average molecular weight of HPP and LPP both decreased with the addition of a nucleating agent. The rotational rheometer and capillary rheometer analysis showed that the effect of NA-21 on reducing intermolecular entanglement was more significant, whether in HPP or LPP. The addition of NA-21 had less elastic energy storage and better flow stability, and could be processed at a higher speed. Simultaneously, the relaxation time in the blends with LPP was shorter than that with HPP. It was found that the crystallinity and nucleation efficiency of HPP/nucleating agent blends increased remarkably, while there was a barely perceptible increase in LPP/nucleating agent blends.

Keywords: polypropylene; molecular weight; organic phosphate nucleating agents; rheology

check for updates

Citation: Li, J.; Liang, Z.; Gao, C.; Luo, S.; Huang, S.; Zhang, D.; Qin, S. The Application of Organic Phosphate Nucleating Agents in Polypropylene with Different Molecular Weights. *Crystals* **2021**, *11*, 1543. https://doi.org/10.3390/cryst11121543

Academic Editors: Andrónico Neira-Carrillo and Dirk Zahn

Received: 29 October 2021
Accepted: 7 December 2021
Published: 10 December 2021

Publisher's Note: MDPI stays neutral with regard to jurisdictional claims in published maps and institutional affiliations.

Copyright: © 2021 by the authors. Licensee MDPI, Basel, Switzerland. This article is an open access article distributed under the terms and conditions of the Creative Commons Attribution (CC BY) license (https://creativecommons.org/licenses/by/4.0/).

1. Introduction

It is well-documented that polypropylene (PP) has excellent properties, such as being non-toxic, odorless, low density and easy to process, as well as having a high chemical resistance. It can replace other expensive engineering thermoplastics and has been widely employed for many industrial applications [1–4]. At the same time, PP products also have the disadvantages of easy shrinkage, sensitivity to ultraviolet radiation and poor transparency [5]. It is known that adding a nucleating agent (NA) is an effective method for obtaining high-performance materials, and that some chemically active NAs can also be used in new construction materials [6]. The impact of the nucleating agents is very critical to the final performance of PP, since they can affect the mechanical, transparency and crystallization properties by changing the crystallization behavior and intermolecular force [7–9].

To date, most studies have focused on the crystal morphology [10,11], crystallization behavior [12], crystal forms [13], crystallization kinetics [14,15] and crystallization rate of PP [16,17] with the nucleating agents. However, the influence of the interaction behavior between the molecular chains of polypropylene and the NA is rarely attended. Rheological analysis is recognized as a good method to characterize the phase behavior of multicomponent blend systems [18–21]. There are many studies on the rheological properties of polymer composite systems. Bendjaouahdou et al. [22] discussed the effect of organoclay on

a polypropylene/natural rubber blend by means of rheology. Grizzuti et al. [23] discussed a new rheological mothed which could obtain reliable viscoelastic properties developed during the crystallization process.

The products under the trade names NA-11 and NA-21 are typical examples of organic phosphate nucleating agents, which are very important type-α phase NAs for PP. The excellent nucleation effect of the organic phosphate has attracted widespread attention in academic circles [24–29]. It has been shown that ADK STAB NA-11 gave the high Tc and stiffness to PP, which was attributed to the optimal epitaxial match between the PP helix and the organophosphate molecules [30,31]. However, the polar portion of the nucleating agent was incompatible with PP and had a higher melting point, resulting in its poor dispersion in PP. NA-21 provides an excellent clarity at lower molding temperatures and has a high nucleation efficiency and, as a result, is popular in industrial applications [32].The works mentioned above have provided a firm foundation for the study of the crystallization properties of the NA/PP blends, and most of the research was only about low melt index PP. The crystallization behavior of a polymer composite can usually be quantified by traditional means, such as XRD, POM and DSC. However, rheological testing is sensitive to the microstructure of composites, and can be used as a powerful means to study the crystallization behavior of polymers as a complement to routine testing.

At present, lots of research has focused on the nucleation efficiency, mechanical properties, simple crystallization behaviors and morphologies of nucleating agents in PP, and most of the it has focused on low melt index PP. To our knowledge, no systematic studies have been carried out on PP with different molecular weights which were nucleated with organic phosphate. In this work, the effect of organic phosphate NAs on rheological behavior, change of molecular weight and crystallization properties of PP with different molecular weights were systematic studied. Our contribution to the study of NAs mixed with PP was to use rheological methods as a means of characterizing the influence of NAs on the intermolecular interactions, molecular chain motion and crystallization behavior of polymer macromolecules. In the work presented here, the capillary rheometer and oscillatory rheometer were evaluated. An analysis of the dispersion of NA was also detailed through a scanning electron microscope (SEM) and transmission electron microscope (TEM). The viscosity curves were then used to link the molecular entanglement and molecular chain motion to the crystallization behavior. We describe some extraordinary findings on the change in viscosity when adding NA-11 and NA-21 into the different molecular weights of the PP matrix. Some evidence suggests that the nucleating agents can act as a softening agent in the polymer melt with high molecular weight PP. NA-21 provides a better dispersity at the same concentration and has a higher nucleation efficiency than that of NA-11.

2. Experimental

2.1. Materials

The high molecular weight polypropylene (HPP), trade name T30S (Lanzhou petrochemical company, Lanzhou, China), has a tacticity of 98%, melt flow rate of 2.6 g/10 min, Mw of 25.6 $\times$ 10^4 g/mol and Mw/Mn = 3.5. The low molecular weight polypropylene (LPP), trade name MN60 (Luoyang petrochemical company, Luoyang, China), has a tacticity of 98%, melt flow rate of 60 g/10 min, Mw of 15.6 $\times$ 10^4 g/mol and Mw/Mn = 2.5. The nucleating agent NA-11, trade name ADK STAB NA-11 (Asahi Denka Co., Ltd., Tokyo, Japan), has a degradation temperature at 5 wt% loss of 442 °C. The nucleating agent NA-21, trade name is ADK STAB NA-21 (Asahi Denka Co., Ltd., Tokyo, Japan), has a degradation temperature at 10 wt% loss of 295 °C.

2.2. Specimen Preparation

HPP, LPP and the NAs were dried in a vacuum oven at 80 °C for 8 h before use. Two kinds of NA/PP blends were prepared in the predetermined weight percentages of 0.2 wt% of the NAs. These two categories were mixed fully and blended in a co-

rotating twin-screw extruder (L/D = 35, Jieya Machine Co., Ltd., Nanjing, China) with a screw speed of 300 rpm. The barrel temperatures were maintained at 160, 170, 180, 190, 200 and 210 °C from hopper to die. The extrudates were injection-molded into 185 mm × 10 mm × 4 mm bars by an injection molding machine (CJ80E, Zhende Machine Co., Ltd., Guangzhou, China). The temperature of the injection molding machine was set at 210 °C/200 °C/190 °C, with an injection time of 5 s and a cooling time of 30 s. Standard specimens were prepared and placed in an incubator for more than 24 h before testing.

2.3. Characterization

2.3.1. Morphological Characterizations

The dispersibility of NA-11 and NA-21 in the PP blend was characterized by a scanning electron microscope (SEM) and transmission electron microscope (TEM). The samples of SEM were immersed in liquid nitrogen for 12 h and then fractured. The fractures were then covered with gold and observed through a Quanta 250 FEG SEM (FEI Company, Hillsboro, WA, USA) at an accelerating voltage of 10 kV.

The TEM specimens of the PP blends were prepared using an LKB-5 microtome (LKB Co., Stockholm, Sweden). Ultrathin sections (60~80 nm) were cut from Izod bars under cryogenic conditions, perpendicular to the flow direction. All samples were observed through a high-resolution TEM (JEM200CX, JEOL, Tokyo, Japan) at an accelerating voltage of 120 kV.

2.3.2. Melt Flow Rate (MFR)

The melt index of the PP blends was tested according to the ASTM 123886T Standard at 220 °C/2.16 kg.

2.3.3. Gel Permeation Chromatograph (GPC)

The average molecular weight (Mn), weight-average molecular weight (Mw) and polydispersity index (PDI) of the PP blends were measured by GPC (Waters, Milford, CT, USA). All the samples were dissolved in trichlorobenzene (TCB) at 150 °C.

2.3.4. Rheological Analysis

Rotational Rheometer

The dynamic rheological analysis of the PP blends was carried out by a rotational rheometer (ARES-G2, TA, New Castle, DE, USA) with an oscillation mode. All the samples were injection molded into the 25 mm diameter disc before testing. The testing temperature was 160 °C and the frequency range was 0.01–100 rad/s with a strain amplitude of 5%. All the tests were performed under a nitrogen environment.

Capillary Rheology

The shear flow behavior of the PP/NA blends was carried out by a capillary rheometer (Acer 2000, TA, New Castle, DE, USA). The testing temperature was set at 190 °C, then certain pellets were weighed, the granules were added into a charging barrel and the granules were compacted in the barrel. After the sample melted, the data was recorded.

2.3.5. Differential Scanning Calorimeter

The crystallization process was studied using a differential scanning calorimeter (Q10, TA, New Castle, DE, USA). All the samples of about 5 mg were heated from 40–250 °C at a heating rate of 10 °C min^{-1}, then the samples were cooled to 40 °C at the same rate.

The crystallinity (*Xc*) of the PP in the blends was determined from the crystallization exotherms by using the following equation

$$Xc = \frac{\Delta H}{(1-\varphi)\Delta H_{100}} \quad (1)$$

where ΔH is the overall enthalpy of the crystallization obtained from the integral area of the cooling thermogram, φ is the volume fraction of the nucleating agent in the composites and ΔH_{100} is the enthalpy of PP of 100% crystallinity and taken as 209 J/g.

3. Results and Discussion

3.1. Morphological Study

The SEM images of the HPP/nucleating agent and LPP/nucleating agent blends are shown in Figure 1. The morphology is obvious for all samples and the size of the nucleating agent particles in the HPP blends are smaller than those in the LPP blends, due to the better compatibility between the nucleating agent and high molecular weight polypropylene. In comparison to NA-11, NA-21 has better dispersion whether in the HPP or LPP matrix (Figure 1b,d), since the particle size of NA-21 in the matrix is smaller than that of NA-11. The increase in the particle size of the droplets is related to the agglomeration of the dispersed phase. This implies that one property of the NA-11 is the tendency to aggregate into compact and dense crystallites [33]. On the contrary, the laurate that is compatible with PP in NA-21 makes the long hydrocarbon chain interact with PP molecules, and the good dispersion of NA-21 also creates more nucleation embryos for the adsorption of polypropylene molecules than NA-11. To further prove the dispersity of the nucleating agent, TEM is employed.

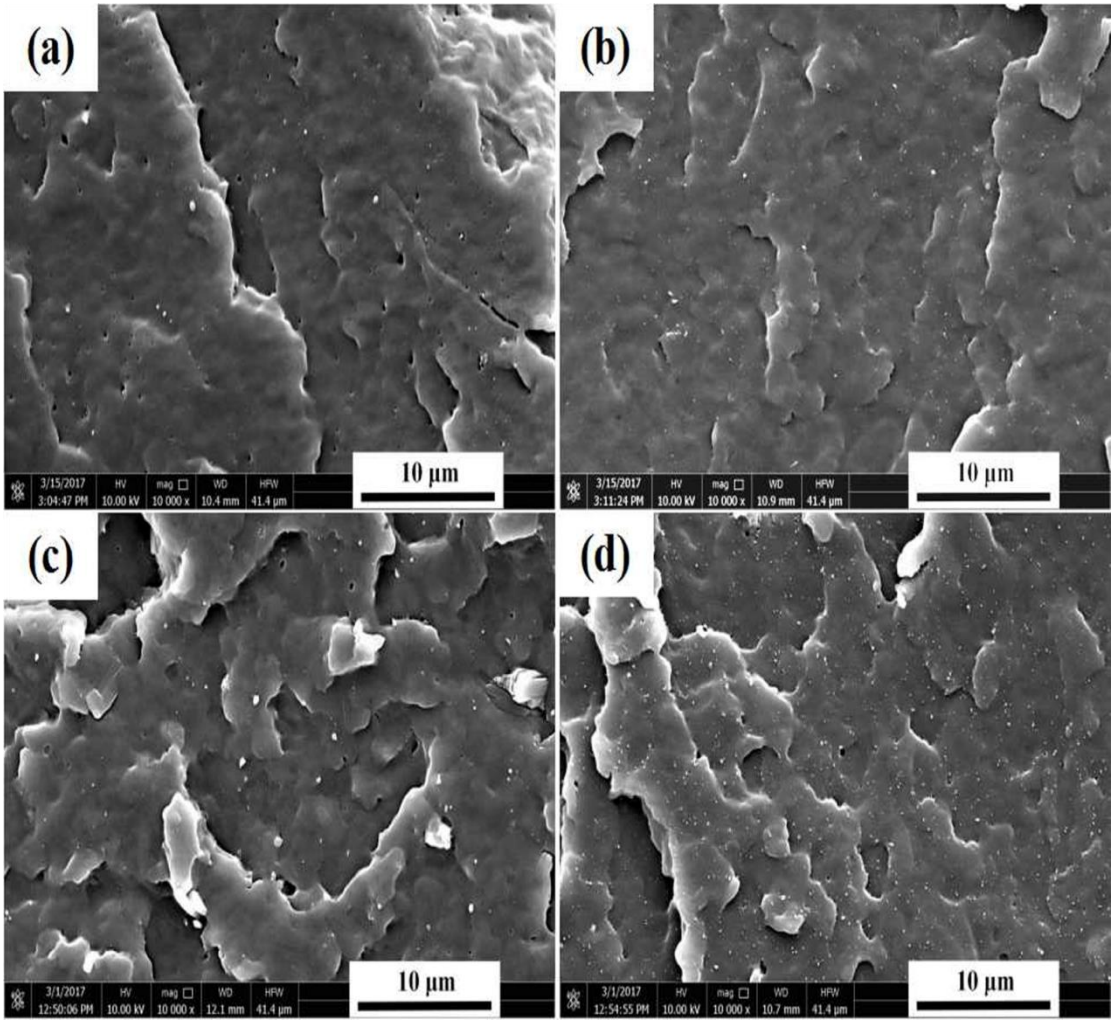

Figure 1. SEM micrographs of the dispersion of the NA in PP with different molecular weights: (**a**) LPP/NA-11, (**b**) LPP/NA-21, (**c**) HPP/NA-11, (**d**) HPP/NA-21.

Seen through the SEM, NA-11 exhibits some obvious agglomeration (Figure 2a,b) and NA-21 particles disperse uniformly in the PP matrix (Figure 2c,d).These results verify that the NA particles have a different dispersive quality in PP. It can be clearly seen from the TEM images that there is a distinct shedding phenomenon for NA-11 particles. The aggregates of NA-11 form strong bonds that could not be broken apart by mechanical methods. The poor dispersion of NA-11 may be because of the disadvantage of the high melting point of NA-11. Compared with NA-11, NA-21 has a lower melting point and is more easily dispersed in the PP matrix. Whichever nucleating agent is used, its dispersion in HPP is better than that of in LPP. Furthermore, the nucleation efficiency of the NA is greatly related to the geometry of itself and its compatibility with the polymer. Hence, this could have a profound impact on the rheology and crystallization properties of PP.

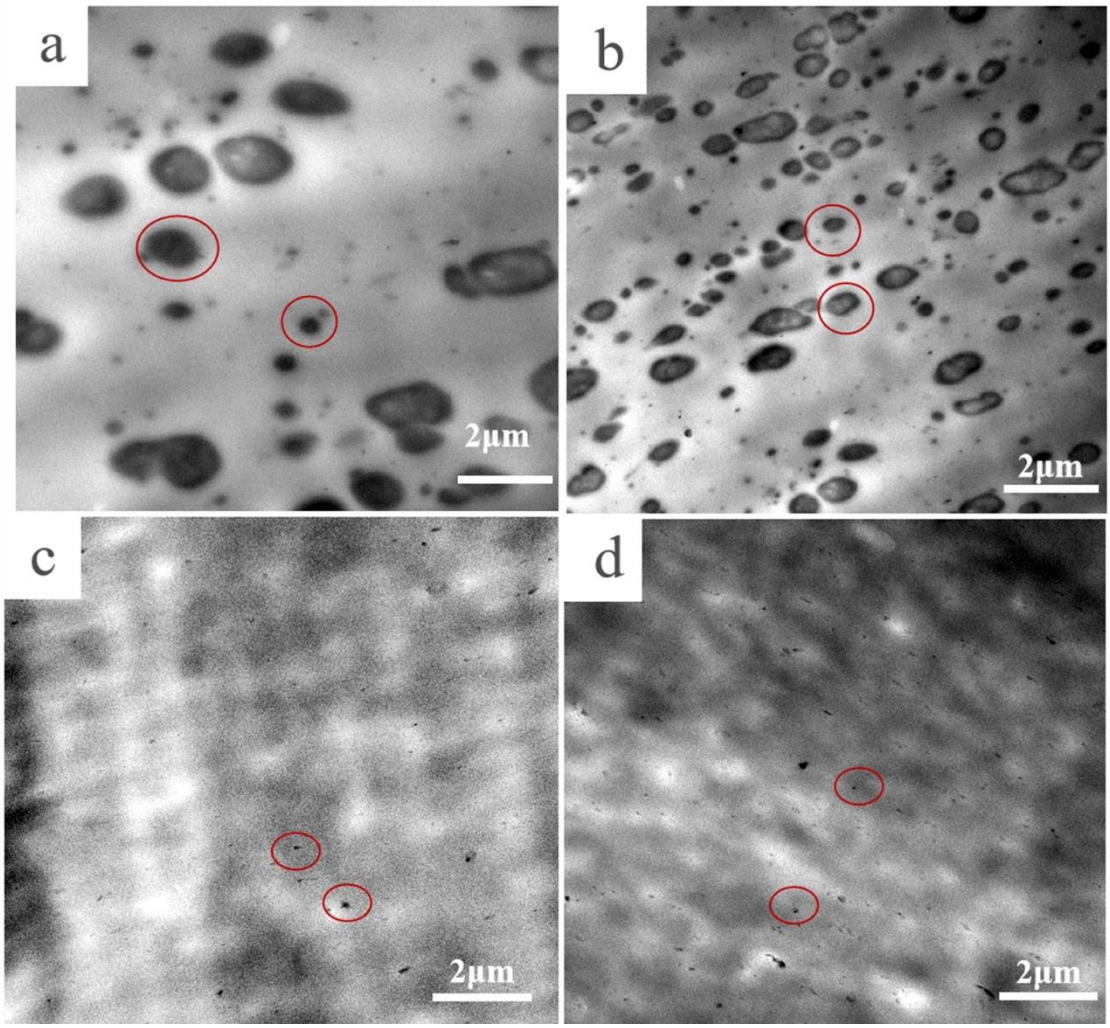

Figure 2. TEM micrographs of the dispersion of the NA in PP with different molecular weights: (**a**) LPP/NA-11, (**b**) HPP/NA-11, (**c**) LPP/NA-21, (**d**) HPP/NA-21.

3.2. Change of Molecular Weight

The results of the MFR, the average molecular weight (Mn), weight-average molecular weight (Mw) and polydispersity index (PDI) of the PP/NA blends are listed in Table 1. Studies have shown that, during melt processing, the polymer macromolecules are subjected to mechanical and thermal stress, which promotes the chemical reaction of the materials, thus causing polymer degradation [34]. The main problems with PP are chain scission and the reduction in polydispersity. As shown in Figure 3C, compared with pure polypropylene, the components of the HPP/nucleating agent blends with ultra-high molecular weights

visibly decrease. Whereas, as shown in the partial enlarged drawing of the cumulative high molecular weight distributions (Figure 4C), the components of the LPP/nucleating agent blends with ultra-high molecular weights decrease slightly. Primarily, the chain entanglements of HPP are stronger than those of LPP. Based on the Bueche mechanical degradation theory [35], the polypropylene degradation during multiple extrusions is thought to be thermomechanical, caused by chain scissions (apparently promoted by the chain entanglements). Secondly, SEM and TEM have previously found that the dispersion of the nucleating agent in the LPP matrix is poor, as the aggregates of the nucleating agent can act as a barrier and hinder polar–polar interaction between PP chains [36]. Therefore, this indicates that the addition of a nucleating agent into a polypropylene matrix where the scission of HPP occurs is more serious.

Table 1. Melt flow index (MFI), molecular weight (number average, weight average, z average) and polydispersity (Mw/Mn) of the pure PP and PP/nucleating agent blends.

Samples	MFI (g/10 min)	Mw (g/mol)	Mn (g/mol)	Mz (g/mol)	Mw/Mn
HPP	2.7	273,381	91,056	565,908	3.00
HPP/NA-11	5.9	239,676	84,364	493,107	2.84
HPP/NA-21	5.3	258,599	97,818	518,524	2.64
LPP	65.8	151,948	53,939	326,923	2.81
LPP/NA-11	72.4	144,440	47,976	314,034	3.01
LPP/NA-21	59.2	149,623	52,078	322,823	2.87

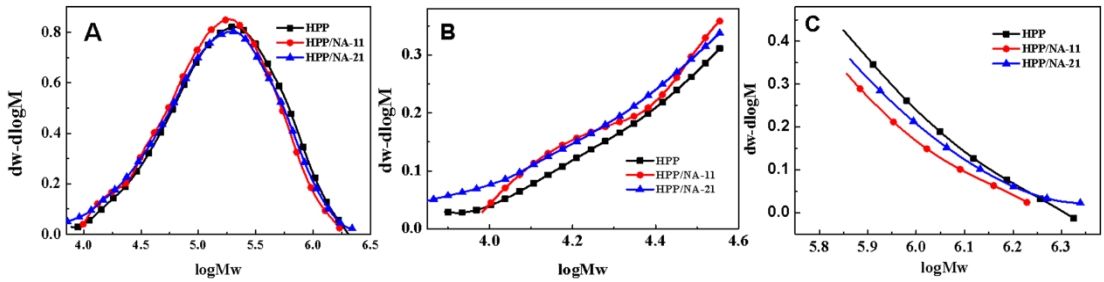

Figure 3. (**A**) cumulative weight distribution curves of HPP and HPP/NA blends; (**B**,**C**) partial enlarged drawing of cumulative low and high molecular weight distributions, respectively.

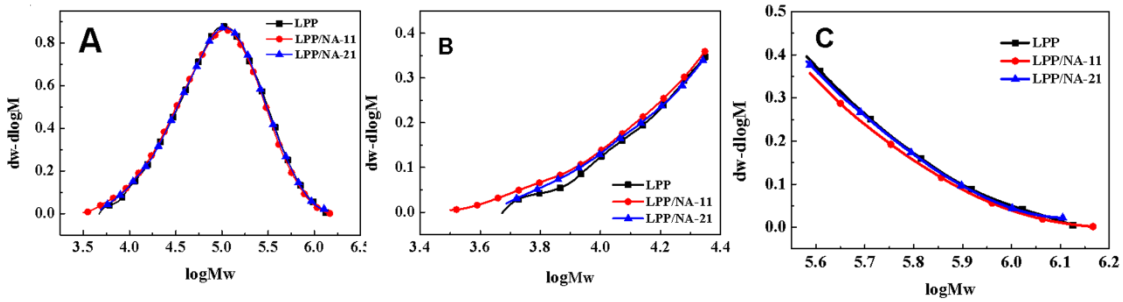

Figure 4. (**A**) cumulative weight distribution curves of LPP and LPP/NA blends; (**B**,**C**) partial enlarged drawing of cumulative low and high molecular weight distributions, respectively.

As shown in Table 1, the Mz of the HPP/nucleating agent blends decrease remarkably, while it shows a significant increase in the Mn of the HPP/NA-21 blend. Lazar M et al. [37] noted that Mz is sensitive to ultra-high molecular weight components, but Mn and Mw are sensitive to moderately high molecular weight components. As shown in Figure 4A, the components of the HPP/NA-11 and HPP/NA-21 blends with high molecular weights decrease definitively (the reduction was 14.1 wt% and 5.7 wt%, respectively). In the LPP/NA system, the Mw decreases slightly. It can be concluded that the degradation of the long molecular chains of HPP results in the decrease in the Mz of the HPP/nucleating

agent blends. Additionally, reactions such as biradical coupling might occur among the macroradicals with low molecular weights, resulting in the increase in the Mn of the HPP/NA-21 blend. On the contrary, the Mn of the HPP/NA-11 blend barely changes. Simultaneously, as shown in Table 1, compared with pure LPP, there is also little change in all the average molecular weights of the LPP/nucleating blends. This result is consistent with our previous analysis. Some authors [38,39] have reported that the melt flow index and molecular weight can be directly correlated (MFI∝1/Mw) for lineal polymers. As shown in Table 1, the melt flow index (MFI) of HPP increases visibly due to the addition of the NA, while the MFI the of LPP/nucleating agent blends increases slightly. The PDI (Mw/Mn) of the HPP/NA-11 and HPP/NA-21 blends are about 5.3% and 12%, respectively, and are lower than those of pure HPP. It is revealed that even the PDI of pure HPP is relatively low (Mw/Mn = 3), and that the ratio of the Mw/Mn of HPP can be further narrowed by introducing a nucleating agent. Since the chain entanglement is stronger in the HPP system, the long chains are more prone to degradation during the melt compounding, resulting in a narrow MWD and low PDI. In contrast, the values of the PDI (Mw/Mn) of LPP/NA-11 and LPP/NA-21 blends increase by 7.1% and 2.1%, respectively, and are still higher than that of pure LPP. As shown in Figure 4A, the concentration of the LPP/NA-11 and LPP/NA-21 blends' molecular weights also decrease slightly.

3.3. Rheological Behaviors

The complex viscosities as a function of the frequency for the HPP/nucleating agent and LPP/nucleating agent blends are shown in Figures 5 and 6, respectively. It is observed that adding the nucleating agent causes an indistinctive shear-thinning behavior, and that the transition from the power-law region to the Newtonian plateau occurs at lower frequencies due to molecular chain disentanglement [40]. In addition, it is obvious that the viscosities of the HPP/nucleating agent blends are all lower than the neat components for chain scission, which is consistent with the molecular weight test results above. However, the viscosity of the HPP/NA-21 blend is lower than that of the HPP/NA-11 blend, since the interaction force between the molecular chains becomes weak due to the addition of NA-11. The sodium laurate components in NA-21 combine with the macromolecular chains through hydrogen bonding, which leads to more negative charge with large molecular chains, electrostatic repulsion and steric hindrance, resulting in the macromolecular stretch and the chain tangles weakening [41]. According to the molecular weight test results, it is also found that the effect of NA-21 on reducing intermolecular entanglement is more significant than NA-11, whether in HPP or LPP.

The linear viscoelastic data for the HPP and LPP blends with different nucleating agents are displayed in Figures 7 and 8. The storage modulus (G') is a response to the reversible elastic deformation and the loss modulus (G'') is a response to irreversible viscous flow. Compared with pure HPP, the G' and G'' values of the HPP/NA blends decrease at a 0.01–100 rad/s frequency range. The slope of the log of G' versus the log of the HPP/NA-11 and HPP/NA-21 blends increases at the terminal region. The result indicates that PP blends with NAs show lower elasticities than those of the HPP matrix. The decrease in elasticity at low frequencies is attributed to the lower stored energy through the intermolecular force between the macromolecular chains. However, the variations of G' and G'' for the LPP/nucleating agent blends seem subtle. The chain segments relax at a 0.01–100 rad/s frequency range and contribute to the viscoelasticity of the whole system, resulting in the viscoelasticity of the blends being not much different from the low molecular weight system of the LPP blends. This phenomenon indicates that the nucleating agent has a larger effect on the molecular chain motion of LPP. The loss tangent ($\tan\delta$) of the LPP and HPP blends has the same trend (Figures 7C and 8C). When the dispersed phase is relatively small, material flows or behaves in a manner similar to a viscous liquid over a longer time scale (at low frequencies) with a correspondingly higher tan value [42]. The results show that NA-21 has better dispersibility than NA-11 in the PP matrix, which is consistent with the results of the electron microscopy above.

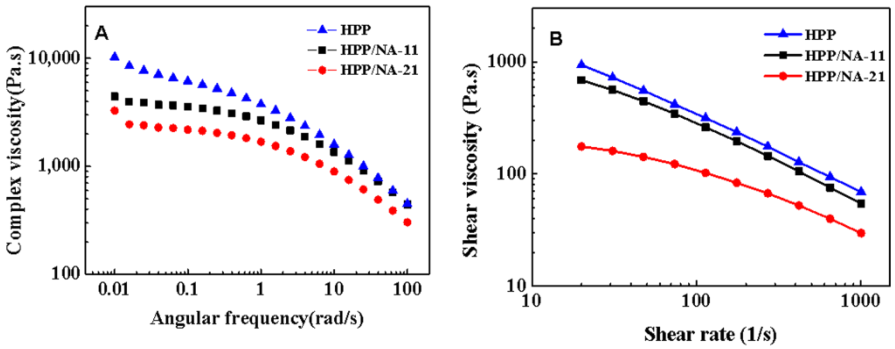

Figure 5. (**A**) Complex viscosity of HPP and HPP/NA blends. (**B**) Shear viscosity of HPP and HPP/NA blends.

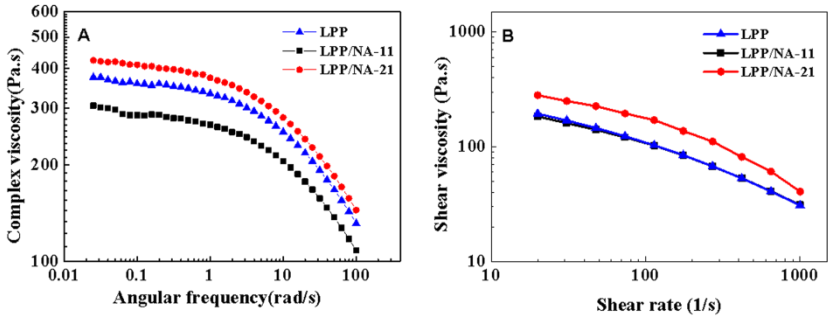

Figure 6. (**A**) Complex viscosity of LPP and LPP/NA blends. (**B**) Shear viscosity of LPP and LPP/NA blends.

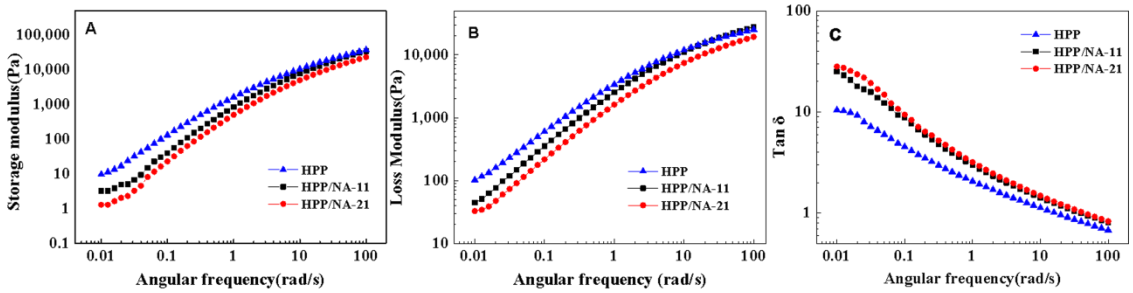

Figure 7. Rheological curves of HPP and HPP/NA blends: (**A**) storage modulus G′, (**B**) loss modulus G″, (**C**) Tanδ plots versus frequency at 175 °C.

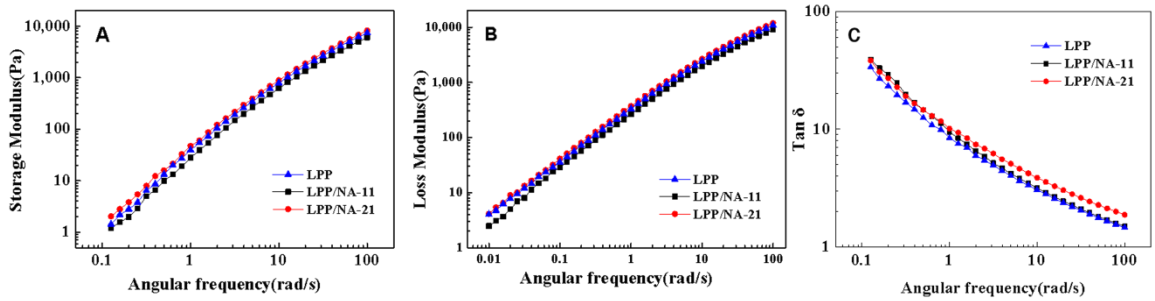

Figure 8. Rheological curves of pure LPP and LPP/NA blends: (**A**) storage modulus G′, (**B**) loss modulus G″, (**C**) Tanδ plots versus frequency at 175 °C.

The weighted relaxation spectrum of the samples at 175 °C are shown in Figure 9A,B. As we all know, the relaxation time spectrum of the polyblends is the result of the interaction of the matrix relaxation time and dispersed phase relaxation time. The curve of HPP or curve of LPP only shows one peak and the value of the x-coordinate (s) corresponding to

this peak is the relaxation time of the pure PP melt. However, the curves of the HPP/NA-11 and HPP/NA-21 blends show two peaks in the weighted relaxation spectra. Therefore, the HPP/NA system has a longer relaxation time than the LPP/NA system, which is associated with the molecular chain disentanglement of the HPP matrix. The molecular weight of the HPP system is large and the microcosmic relaxation of the system is difficult, so the characteristic relaxation time is longer than in the LPP system. The pure HPP has the unique value of 1.78 s, the values of the HPP/NA-11 and HPP/NA-21 blends are shifted toward to 0.71 s and 0.56 s, respectively. On the other hand, NA-21 is a kind of compound nucleating agent, which is mainly composed of aromatic heterocyclic phosphate aluminum and carboxylate. The long chain carboxylic acid acts as a compatibilizer in the PP matrix, and the relaxation time of the interface can be significantly reduced. At the same extrusion speed, the system with the added NA-21 has less elastic energy storage and better flow stability, and could be processed at a higher speed.

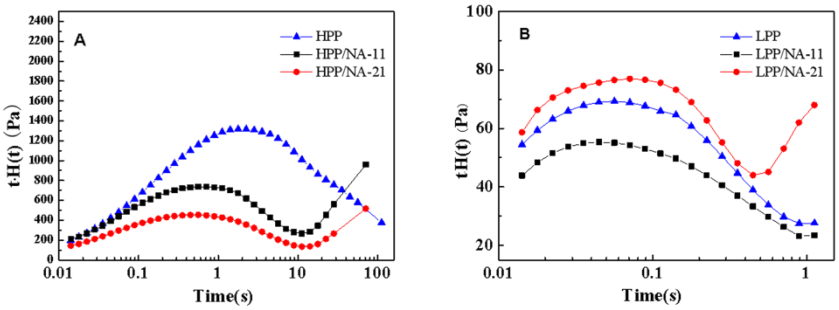

Figure 9. (**A**) Weighted relaxation spectra of HPP and HPP/NA blends at 175 °C. (**B**) Weighted relaxation spectra of LPP and LPP/NA blends at 175 °C.

In the polymeric systems, a Cole–Cole plot is one of the main ways to represent the homogeneity and compatibility of the different substances. As shown in Figure 10, a single circular arc of the Cole–Cole curve represents a homogeneous melt system. Through further analysis of the Cole–Cole curve of the iPP composite material in Figure 10, it is found that the radius of the Cole–Cole curve decreases with the addition of a nucleating agent and with the presence of NA-21 the radius decreases further, indicating that the compatibility of the system is better [21].

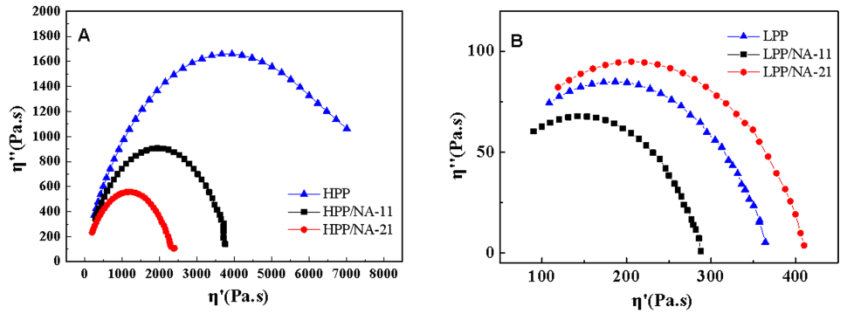

Figure 10. (**A**) Cole–Cole plots of HPP and HPP/NA blends at 175 °C.(**B**) Cole–Cole plots of HPP and HPP/NA blends at 175 °C.

From the discussion above, it is clear that the effect of different organophosphate nucleating agents on the microstructure of PP can be reasonably followed by rheological measurements which are much sensitive to the microstructural changes.

3.4. Thermal Characterization

Figure 11 shows the DSC cooling curves of the samples of HPP and LPP blends in all thermograms. For the HPP blends (Figure 11A), the Tc of HPP/NA-11 and HPP/NA-21 has increased by 13.2 °C and 14.7 °C compared with HPP. Simultaneously, the crystallinity

increases to 47.80% and 51.15%, indicating that the nucleation effect of the nucleating agent for the HPP matrix is remarkable. However, for the LPP blends, the Tc of LPP/NA-11 and LPP/NA-21 has increased by 3.69 °C and 3.08 °C compared with LPP. Simultaneously, the crystallinity of LPP/NA also increases. The crystalline parameters of the HPP and LPP blends are shown in Table 2. It is clear that the ability of the nucleating agent to promote the crystallization of high molecular weight polypropylene is superior to the low molecular weight polypropylene.

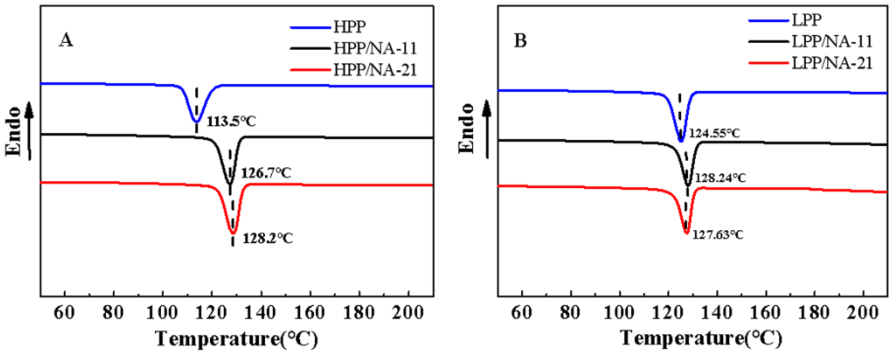

Figure 11. (**A**) DSC cooling thermographs of HPP and HPP/NA blends. (**B**): DSC cooling thermographs of LPP and LPP/NA blends.

Table 2. Crystalline parameters of the PP and PP/NA blends.

Sample	T_c/°C	T_m/°C	H_m/(J·g^{-1})	X_c(%)
HPP	113.50	163.93	92.97	44.48
HPP/NA-11	126.70	166.16	99.91	47.80
HPP/NA-21	128.20	165.25	106.90	51.15
LPP	124.55	160.94	91.47	43.77
LPP/NA-11	128.24	161.59	95.75	45.81
LPP/NA-21	127.63	160.26	97.48	46.64

It has been reported that organophosphate nucleating agents play the role of heterogeneous nucleation in the PP blends, which promotes the crystal nucleation and accelerates the crystallization rate of PP. Due to the good dispersion of NA-21, more nucleation sites were created for PP. The NA-21 nucleating agent accelerates the adsorption of molecular chain segments and enhances the stacking and diffusion rates of the crystal nuclei. The stronger the adsorption of the nucleating agent is, the easier the molecular chain segment diffuses into the surface of the crystal nucleus to accumulate and grow, and the faster the chain segment moves and diffuses into the crystal nucleus. That is, the faster the crystallization rate, the higher the crystallization temperature.

4. Conclusions

In this work, two kinds of organic phosphate nucleating agent (NA-11 and NA-21) were used in PP with different molecular weights through the melt extrusion method. The polar portion in NA-11 was incompatible with PP and had a higher melting point than PP. Compared with NA-11, NA-21 had a lower melting point and was more easily dispersed in the PP matrix. The good dispersion of NA-21 created more nucleation embryos for the adsorption of polypropylene molecules than the agglomerated NA-11. The gel permeation chromatography (GPC) analysis showed that the average molecular weight of HPP and LPP both decreased with the addition of an NA. First of all, the PP/NA blends prepared by melt compounding led to chain scission. On the other hand, the molecular chain entanglement of HPP became stronger, so the chain scission was more serious. The rotational rheometer and capillary rheometer analysis showed the effect of NA-21 on reducing intermolecular entanglement was more significant, whether in HPP or LPP. The addition of NA-21 had less elastic energy storage and better flow stability, and could be processed at a higher speed.

Simultaneously, the relaxation time in the blends with LPP was shorter than that with HPP blends. The nucleating agents could significantly improve the crystallization behavior of high molecular weight polypropylene. In total, NA-21 provided better dispersity at the same concentration and had a higher nucleation efficiency than that of NA-11 in both LPP and HPP blends.

Author Contributions: Conceptualization, S.Q.; Methodology, J.L.; Data analysis, S.L. and Z.L.; Data curation, C.G. and S.H.; Writing—original draft preparation, J.L.; Writing—review and editing, D.Z.; Funding acquisition, J.L. and S.Q. All authors have read and agreed to the published version of the manuscript.

Funding: This research was funded by National Natural Science Foundation of China, Grant No. 51863004, 52063007; The Science and Technology Planning Project of Guizhou Province, Grant No. [2021]9, [2020]4Y223, [2020]4Y226, [2019]2029; The Talent Cultivation Project of Guizhou Province, Grant No. [2019]5630, [2020]6024.

Institutional Review Board Statement: Not applicable.

Informed Consent Statement: Not applicable.

Data Availability Statement: Not applicable.

Conflicts of Interest: The authors declare no conflict of interest.

References

1. Markus, B.; Sandra, G.; Doris, H.; Hans, W.S.; Magnus, K.; Paul, S.; Klaus, S.; Dietmar, M.; Kurt, H. "Designer" Nucleating Agents for Polypropylene. *Macromolecules* **2005**, *38*, 3688–3695.
2. Zoe, V.Q.J.; Carlos, A.; Blanca, E.C.; José, M.B.H. Effect of Sorbitol Templates on the Preferential Crystallographic Growth of Isotactic Polypropylene Wax. *Crystals* **2018**, *8*, 59.
3. Roberto, S.; Marcel, S.; Christian, H. Simulation of crystallization of isotactic polypropylene with different shear regimes. *Thermochim. Acta* **2018**, *10*, 44–54.
4. Li, J.; Long, L.J.; He, W.-T.; Zhang, K. Crystallization Behavior and Mechanical Properties of Nanosilica-Reinforced Isotactic Polypropylene Composites. *Intern. Polym. Process.* **2015**, *30*, 542–547. [CrossRef]
5. Sowinski, P.; Piorkowska, E.; Boyer, S.; Haudin, J. Nucleation of crystallization of isotactic polypropylene in the gamma form under high pressure in nonisothermal conditions. *Eur. Polym. J.* **2016**, *85*, 564–574. [CrossRef]
6. Bartosz, S.; Grzegorz, L.G. Improvement of Strength Parameters of Cement Matrix with the Addition of Siliceous Fly Ash by Using Nanometric C-S-H Seeds. *Energies* **2020**, *13*, 6734.
7. Jiang, X.; Zhao, S.; Meng, X.; Xin, Z. Effect of the Metal Phenylphosphonates on the Nonisothermal Crystallization and Performance of Isotactic Polypropylene. *J. Polym. Sci. Part B Polym. Phys.* **2019**, *57*, 161–173. [CrossRef]
8. Hou, W.M.; Liu, G.; Zhou, J.J. The influence of crystal structures of nucleating agents on the crystallization behaviors of isotactic polypropylene. *Colloid Polym. Sci.* **2006**, *285*, 11–17. [CrossRef]
9. Carolus, H.R.M.; Wilsens, L.G.D.H.; Enrico, M.T.; Daniel, H.M.; Gijs, K.; Nils, L.; Ketie, S.; Gerrit, W.M.P.; Sanjay, R. Effect of Self-Assembly of Oxalamide Based Organic Compounds on Melt Behavior, Nucleation, and Crystallization of Isotactic Polypropylene. *Macromolecules* **2018**, *51*, 4882–4895.
10. An, Y.J.; Wang, S.H.; Li, R.; Shi, D.Z.; Gao, Y.X.; Song, L. Effect of different nucleating agent on crystallization kinetics and morphology of polypropylene. *ePolymers* **2019**, *19*, 32–39. [CrossRef]
11. Zhu, P.W.; Edward, G. Distribution of shish-kebab structure of isotactic polypropylene under shear in the presence of nucleatinga-gent. *Macromolecules* **2004**, *37*, 2658–2660. [CrossRef]
12. Zhao, S.C.; Yu, X.; Gong, H.Z. The crystallization behavior of isotactic polypropylene induced by a novel antinucleating agent and its inhibition mechanism of nucleatione. *Ind. Eng. Chem. Res.* **2015**, *54*, 7650–7657. [CrossRef]
13. Yang, Y.; Liang, R.; Chen, Y.; Zhang, C.; Zhang, R.; Wang, X.; Kong, R.; Chen, Q. Using a Self-Assemblable Nucleating Agent to Tailor Crystallization Behavior, Crystal Morphology, Polymorphic Crystalline Structure, and Biodegradability of Poly(1,4-butyleneadipate). *Ind. Eng. Chem. Res.* **2017**, *56*, 7910–7919. [CrossRef]
14. Zhao, W.Y.; Huang, Y.J.; Liao, X.; Yang, Q. The molecular structure characteristics of long chain branched polypropylene and its effects on non-isothermal crystallization and mechanical properties. *Polymer* **2013**, *54*, 1455–1462. [CrossRef]
15. Mubarak, Y.; Harkin-Jones, E.M.A.; Martin, P.J.; Ahmad, M. Modeling of non-isothermal crystallization kinetics of isotactic polypropylene. *Polymer* **2001**, *42*, 3171–3182. [CrossRef]
16. Drongelen, M.; Erp, T.B.V.; Peters, G.W.M. Quantification of non-isothermal, multi-phase crystallization of isotactic polypropylene: The influence of cooling rate and pressure. *Polymer* **2012**, *53*, 4758–4769. [CrossRef]
17. Deshmukh, Y.S.; Wilsens, C.H.R.M.; Leoné, N.; Portale, G.; Harings, J.A.W.; Rastogi, S. Melt-Miscible Oxalamide BasedNucleating Agent and Their Nucleation Efficiency in Isotactic Polypropylene. *Ind. Eng. Chem. Res.* **2016**, *55*, 11756–11766. [CrossRef]

18. Asteasuain, M.; Sarmoria, C.; Brandolin, A. Controlled rheology of polypropylene: Modeling of molecular weight distributions. *J. Appl. Polym. Sci.* **2010**, *88*, 1676–1685. [CrossRef]
19. Sugimoto, M.; Masubuchi, Y.; Takimoto, J. Melt rheology of polypropylene containing small amounts of high molecular weight chain. I. Shear flow. *J. Polym. Sci. Part B Polym. Phys.* **2001**, *39*, 2692–2704. [CrossRef]
20. Abbasi, F.; Tavakoli, A.; Razavi Aghjeh, M.K. Rheology, morphology, and mechanical properties of reactive compatibilized polypropylene/polystyrene blends via Friedel–Crafts alkylation reaction in the presence of clay. *J. Vinyl Addit. Technol.* **2018**, *24*, 18–26. [CrossRef]
21. Ardakani, F.; Jahani, Y.; Morshedian, J. The impact of viscoelastic behavior and viscosity ratio on the phase behavior and morphology of polypropylene/polybutene blends. *J. Vinyl Addit. Technol.* **2015**, *21*, 94–101. [CrossRef]
22. Ivonne, O.N.; Milad, K.; Mohammad, A.; Uttandaraman, S. Morphology Evolution, Molecular Simulation, Electrical Properties, and Rheology of Carbon Nanotube/Polypropylene/Polystyrene Blend Nanocomposites: Effect of Molecular Interaction between Styrene-Butadiene Block Copolymer and Carbon Nanotube. *Polymers* **2021**, *13*, 230.
23. Bendjaouahdou, C.; Bensaad, S. Properties of polypropylene/(natural rubber)/organo montmorillonite nanocomposites prepared by melt blending. *J. Vinyl Addit. Technil.* **2011**, *17*, 48–57. [CrossRef]
24. Kilic, A.; Shim, E.; Yeom, B.Y.; Pourdeyhimi, B. Effect of DMDBS (3:2,4-bis(3,4-dimethyldibenzylidene) sorbitol) and NA11(sodium 2,2-methylene-bis (4,6-di-tertbutylphenyl)-phosphate) on electret properties of polypropylene Filaments. *J. Appl. Polym. Sci.* **2013**, *130*, 2068–2075. [CrossRef]
25. Long, L.J.; He, W.T.; Zhang, M.M.; Zhang, K.; Qin, S.H.; Yu, J. Nucleation effects of sodium and ammonium salts of 2, 2′-methylene-bis-(4, 6-di-t-butylphenylene) phosphate in isotactic Polypropylene. *Polym. Eng. Sci.* **2015**, *55*, 22–28. [CrossRef]
26. Long, L.J.; He, W.T.; Li, J.; Xiang, Y.S. Joint effects of molecular structure and crystal morphology of organophosphate monovalent salts on nucleated isotactic poly(propylene). *J. Polym. Res.* **2016**, *23*, 206. [CrossRef]
27. Li, J.; Qin, S.H.; He, W.T.; Xiang, Y.S. The effect of hybrid nucleating agent with silica sol as the supporter on the crystallization behavior and mechanical properties of isotactic polypropylene. *J. Polym. Eng.* **2015**, *35*, 565–573. [CrossRef]
28. Huang, W.J.; Wentao, H.H.; Jie, Y. Synthesis, Characterization and Application of 2, 2′- methylene- bis (4, 6-di-tert-butyl-phenyl) Phosphate Sodium. *Adv. Mater. Res.* **2013**, *834–836*, 119–123. [CrossRef]
29. Zhang, Y.F.; Zhou, P.Z.; Li, Y. The influences of α/β compound nucleating agents based on octamethylenedicarboxylic dibenzoyl-hydrazide on crystallization and melting behavior of isotactic polypropylene. *Polym. Adv. Technol.* **2019**, *30*, 1777–1788. [CrossRef]
30. Zhang, Y.F.; Mao, J.J.; Zhou, P.Z. The relation between chemical structure of dicarboxylic dihydrazide compounds and nucleation effect in isotactic polypropylene. *J. Therm. Analy. Calorim.* **2021**, *145*, 2379–2387. [CrossRef]
31. Wang, B.; Utzeri, R.; Castellano, M.; Stagnaro, P.; MÃller, A.J.; Cavallo, D. Heterogeneous Nucleation and Self-Nucleation of Isotactic Polypropylene Microdroplets in Immiscible Blends: From Nucleation to Growth-Dominated Crystallization. *Macromolecules* **2020**, *53*, 5980–5991. [CrossRef]
32. Zhang, Y.F.; He, B.; Zhou, H.H.; Guo, L.H. Isothermal Crystallization of Isotactic Polypropylene Nucleated with a Novel Aromatic Heterocyclic Phosphate Nucleating Agent. *J. Macromol. Sci. Part B* **2017**, *56*, 811–820. [CrossRef]
33. Vladimirov, V.; Betchev, C.; Vassiliou, A. Dynamic mechanical and morphological studies of isotactic polypropylene/fumed silica nanocomposites with enhanced gas barrier properties. *Compos. Sci. Technol.* **2006**, *66*, 2935–2944. [CrossRef]
34. González-González, V.A.; Neira-Velázquez, G.; Angulo-Sánchez, J.L. Polypropylene chain scissions and molecular weight changes in multiple extrusion. *Polym. Degrad. Stab.* **1998**, *60*, 33–42. [CrossRef]
35. Bueche, F. Mechanical degradation of high polymers. *J. Appl. Polym. Sci.* **1960**, *4*, 101–106. [CrossRef]
36. Hassani, A.J. Preparation and characterization of polyamide 6 nanocomposites using MWCNTs based on bimetallic Co-Mo/MgO catalyst. *Express Polym. Lett.* **2014**, *8*, 177–186. [CrossRef]
37. Lazár, M.; HrcKová, L.; Borsig, E. Course of degradation and build-up reactions in isotactic polypropylene during peroxide decomposition. *J. Appl. Polym. Sci.* **2015**, *78*, 886–893. [CrossRef]
38. Tzoganakis, C.; Vlachopoulos, J.; Hamielec, A.E. Production of controlled-rheology polypropylene resins by peroxide promoted degradation during extrusion. *Polym. Eng. Sci.* **2010**, *28*, 170–180. [CrossRef]
39. Bremner, T.; Rudin, A.; Cook, D.G. Melt flow index values and molecular weight distributions of commercial thermoplastics. *J. Appl. Polym. Sci.* **1990**, *41*, 1617–1627. [CrossRef]
40. Gui, Z.Y.; Wang, H.R.; Gao, Y. Morphology and melt rheology of biodegradable poly(lactic acid)/poly(butylene succinate adipate) blends: Effect of blend compositions. *Iran. Polym. J.* **2012**, *21*, 81–89. [CrossRef]
41. Wang, Y. Role of surfactant molecular weight on morphology and properties of functionalized graphite oxide filled polypropylene nanocomposites. *Express Polym. Lett.* **2014**, *8*, 881–894. [CrossRef]
42. Kashiwagi, T.; Mu, M.; Winey, K. Relation between the viscoelastic and flammability properties of polymer nanocomposites. *Polymer* **2008**, *49*, 4358–4368. [CrossRef]